DOI https: //doi. org/10.1007/s11595-021-2373-2

Molecular Dynamic Regulation of Na and Mg Ions on Lithium Carbonate Crystallisation in Salt Lakes

MA Yanfang[1,2,3,4], XIANG Shaoji[4,5], CUI Zhenhua[4,5], LI Kanshe[3*], ZHANG Zhihong[1,2,4]

(1. Key Laboratory of Comprehensive and Highly Efficient Utilization of Salt Lake Resources, Qinghai Institute of Salt Lakes, Chinese Academy of Sciences, Xining 810008, China; 2. Qinghai Province Key Laboratory of Resources and Chemistry of Salt Lakes, Xining 810008, China; 3. Chemistry and Chemical Engineering College of Xi'an University of Science and Technology, Xi'an 710054, China; 4. Innovation Academy for Green Manufacture, Chinese Academy of Sciences, Beijing 100190, China; 5. Key Laboratory of Organofluorine Chemistry, Shanghai Institute of Organic Chemistry, University of Chinese Academy of Sciences, Chinese Academy of Sciences, Shanghai 200032, China)

Abstract: Lithium carbonate (Li_2CO_3) was synthesised by adding sodium (Na) and magnesium (Mg) ions into a lithium chloride solution at different concentrations, followed by the addition of an appropriate sodium carbonate solution. Then, the morphology, purity and particle size of Li_2CO_3 crystals were investigated. The Na and Mg ions had negligible and remarkable effects, respectively, on the product purity; however they both greatly influenced its morphology. Their effects on the nucleation and growth rates, the radial distribution function and the diffusion behaviour of the synthesised Li_2CO_3 were investigated via molecular dynamics methods; the Na ions slowed down the crystal nucleation and growth rates, while the Mg ions accelerated them. Moreover, the Mg ions rendered the system short-range ordered and long-range disordered and also increased the diffusion coefficient. The results of this study showed that Mg ions are one of the most important factors influencing the purity and yield of Li_2CO_3.

Key words: sodium; magnesium; purity; particle size; diffusion coefficient; analytical kinetics

1 Introduction

Salt lake brines account for 61.8% of the global lithium (Li) resources[1-3]. As natural brines with high lithium content are important Li resources, the salt lake lithium extraction industry is emerging[4-7]. However, due to factors such as the low comprehensive utilization of salt lake resources and the inadequate impurity removal rate in the purification process, lithium carbonate (Li_2CO_3) products exhibit small particle size, large specific surface, severe agglomeration, mother liquor entrainment and peritectic nature. Their purity and specific impurities cannot meet the requirements of the Li battery industry; this severely restricts the development of the salt lake lithium extraction industry. The high-tech field currently presents strict requirements pertaining to the Li_2CO_3 purity and there are new morphology and particle size requisites as well[8-11]. Therefore, the role of the impurities in the Li_2CO_3 crystallisation is particularly important.

Brines of interest for Li extraction have a complex solution chemistry with different concentrations of Na^+, Mg^{2+}, K^+, Cl^-, SO_4^{2-} and $B_4O_7^{2-}$。 The formation of ion pairs between the constituents of other oxyanion-bearing mineral phases, such as $MgCO_3{\cdot}3H_2O$, has been shown to significantly change the ability of the mineral, meanwhile, dissolved ions can form direct interactions with different surfaces on a growing crystal, influencing the stability of the surface and grow[12].

Subsequent to the deep decontamination of the Lithium-rich brine in salt lakes, trace impurities, such as boron and Mg, in the raw material solution for Li precipitation affect the purity of the resulting Li_2CO_3 crystals. In addition, as the Li extraction from salt lake brine for the Li_2CO_3 precipitation used the Li^+, Na^+, Cl^-, CO_3^{2-}–H_2O quaternary system, the effects of the Na ions on the solubility, morphology, particle size and purity of Li_2CO_3 during the crystallisation of Li_2CO_3 cannot be ignored. It is very necessary for molecular dynamics simulations on the crystallization of simulation Na and Mg ions on lithium carbonate crystallisation. Thus, the role of impurity ions in complex crystal-

(Received: July 27, 2020; Accepted: Oct. 18, 2020)

MA Yanfang(马艳芳): Assoc. Researcher; E-mail: mayanfang@sl.ac.cn

*Corresponding author: LI Kanshe(李侃社): Assoc. Prof.; Ph D; E-mail: likanshe@xust.edu.cn

Funded by the 2017 CAS "Light of West China" Program, Innovation Academy for Green Manufacture, CAS (No. IAGM2020C01), Key R&D and Transformation Projects in Qinghai Province(No.2019-GX-167)

line systems must be investigated.

2 Experimental

Lithium solutions with different (separate) concentrations of Na and Mg ions were prepared (Tables 1 and 2). As a raw material solution for research, these were added with a Na carbonate solution to prepare Li_2CO_3 crystals. Then, the effects of the Na and Mg ions on the Li_2CO_3 crystallisation process and its purity were investigated.

Table 1 Lithium solutions containing sodium (Na) ions

No/	N-1	N-2	N-3	N-4	N-5
Li/(mol/L)	3.641	3.134	3.171	3.199	3.547
Na/(mol/L)	0.023	0.147	0.641	1.270	1.421
Cl/(mol/L)	3.997	3.628	4.228	4.968	5.599

Table 2 Lithium solutions containing magnesium (Mg) ions

No.	M-1	M-2	M-3	M-4	M-5
Li/(mol/L)	4.064	4.054	4.061	4.039	4.004
Mg/(mol/L)	0.179	0.346	0.696	1.017	1.342
Cl/(mol/L)	4.559	4.818	5.543	6.141	6.827

3 Results and discussion

3.1 Purity, morphology and particle size

Tables 3 and 4 list the lithium content and the purity of the various Li_2CO_3 crystals prepared by the reaction.

Table 3 Li content and purity of the Li_2CO_3 crystals synthesized using Na

No.	N-S-1	N-S-2	N-S-3	N-S-4	N-S-5
Li/%	18.731	18.600	18.425	18.171	18.037
Purity/%	98.8	98.2	97.2	95.6	95.2

Table 4 Li content and purity of Li_2CO_3 crystals synthesized using Mg

No.	M-S-1	M-S-2	M-S-3	M-S-4	M-S-5
Li/%	16.807	14.148	12.894	12.099	8.046
Purity/%	88.7	74.7	68.0	63.8	42.5

These results show that the presence of the Na and Mg ions directly affected the Li_2CO_3 purity, which decreased as their concentration increased. However, the influence of the Na ions was much smaller than that of the Mg ones.

Fig.1 compares the scanning electron microscopy (SEM) images of the Li_2CO crystals prepared with different concentrations of Na and Mg ions in the raw material solution; the Mg ions directly influenced the product morphology, resulting in poor particle dispersion and a staggered distribution of large and small crystals. Lithium carbonate forms polycrystalline crystals, and Mg ions form a magnesium hydroxide colloid. The appearance of lithium carbonate was changed by complexation and adsorption.

The X-ray diffraction patterns of the Li_2CO crystals (Fig.2) revealed that the increase in the Na and Mg ions concentrations gradually reduced the intensity of the Li_2CO_3 diffraction peaks, indicating a decrease in the purity and Li content. The strongest absorption peak of lithium carbonate occurs at 31°-32°. As the content of sodium and magnesium ions in the system increased, the absorption peak gradually decreased. The reason is that the microcrystalline structure of lithium carbonate has changed. There are many defects in lattice structure.

Fig.3 illustrates the influence of Na and Mg ions on the particle size distribution of Li_2CO_3 products, showing that the presence of Na ions slowed down the nucleation and growth rates. Moreover, the presence of Mg ions induced the crystal agglomeration, broadened

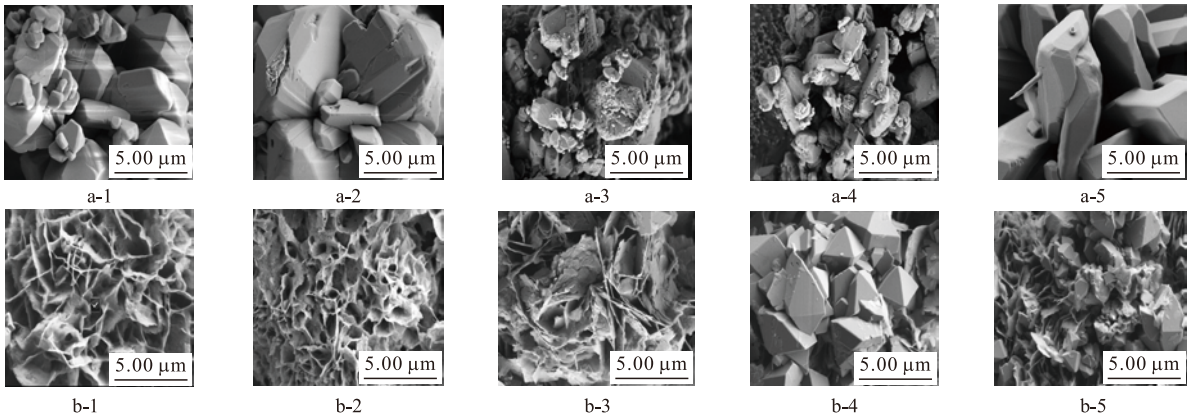

Fig.1 Scanning electron microscopy images of the Li_2CO_3 crystals synthesized in the presence of (a) Na and (b) Mg ions

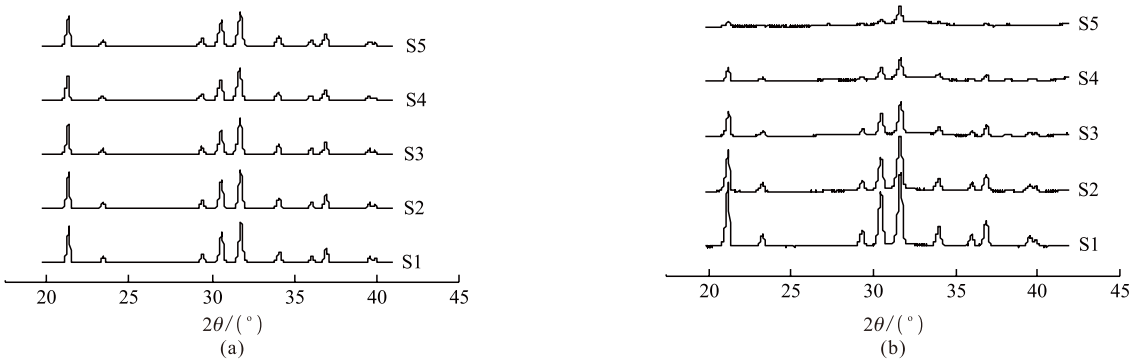

Fig.2 X-ray diffraction spectra of the Li_2CO_3 crystals synthesized in the presence of (a) Na and (b) Mg ions

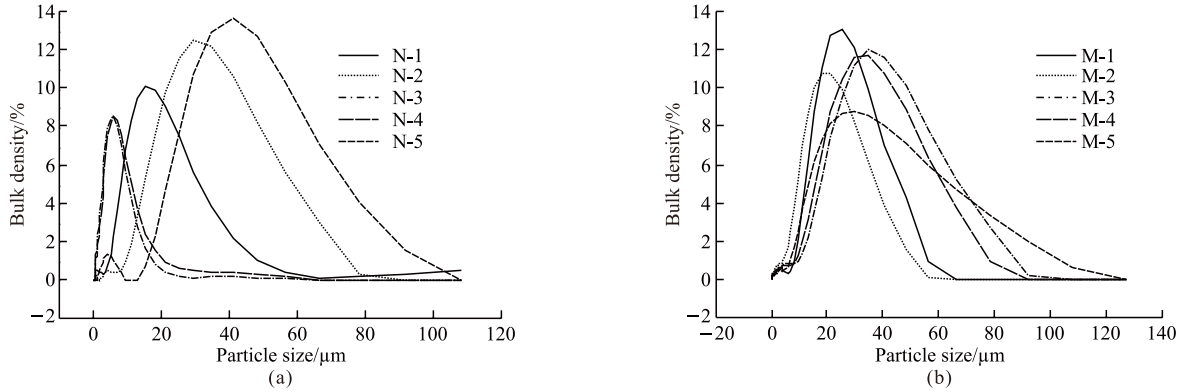

Fig.3 Size distribution of the Li_2CO_3 crystals synthesized in the presence of (a) Na and (b) Mg ions

the particle size distribution and reduced both the average particle size and bulk density. There was no clear regularity between the average particle size of the Li_2CO_3 crystals and the Na and Mg contents, which needs further investigation.

3.2 Molecular dynamics simulation

3.2.1 Simulation method

All the molecular dynamics simulations were performed with the AmberTools 18 package; the general AMBER force field and the TIP3P (transferable intermolecular potential with three points) water model were used for the ions and water, respectively. Subsequent to 2 000 cycles of energy minimization, the models(four simulation systems) were heated to 353 K within 200 ps in the NVT manner, followed by an NPT equilibration for 6 ns. All trajectories involved in the work of trajectories were visualized and analysed by the Visual Molecular Dynamics program; For simulation system, each system has about 6 000 atoms and about 2 000 water molecules. The number of other ions is given by the concentration. Force field is GAFF, and the distance cut-off for the dynamical bond was set to 1.9 Å [13–17].

The impurity effect in the crystallisation process can be divided into two categories: harmful impurities and insignificant impurity effects [18–20]. However, the quantitative relationship between impurities and crystal properties is very lacking and therefore, the action mechanism of the impurities in the Li_2CO_3 crystallisation must be simulated. Four systems were modelled to investigate the properties of Li_2CO_3 crystals formed in the presence of Na and Mg ions. Table 5 summarises the simulation parameters used. The nucleation and growth rates were derived from the first-order kinetics of the free lithium ions concentration with time before and after, respectively the nucleation number stabilisation.

Table 5 Chemical composition of the four simulated systems

No.	Total content /(mol/L)	Chemical composition/(mol/L)			
		Li^+	CO_3^{2-}	Na^+	Mg^{2+}
System1	7.91	4.25	2.58	1.08	0
System2	9.52	4.25	2.58	2.69	0
System3	7.28	4.25	2.58	0.43	0.025
System4	7.29	4.25	2.58	0.21	0.25

The initially established structural model of the system is shown in Fig.4.

3.2.2 Impurity effect on the nucleation and growth rates

The simulations revealed that the nucleation and growth rates of Li_2CO_3 crystals increase in the presence

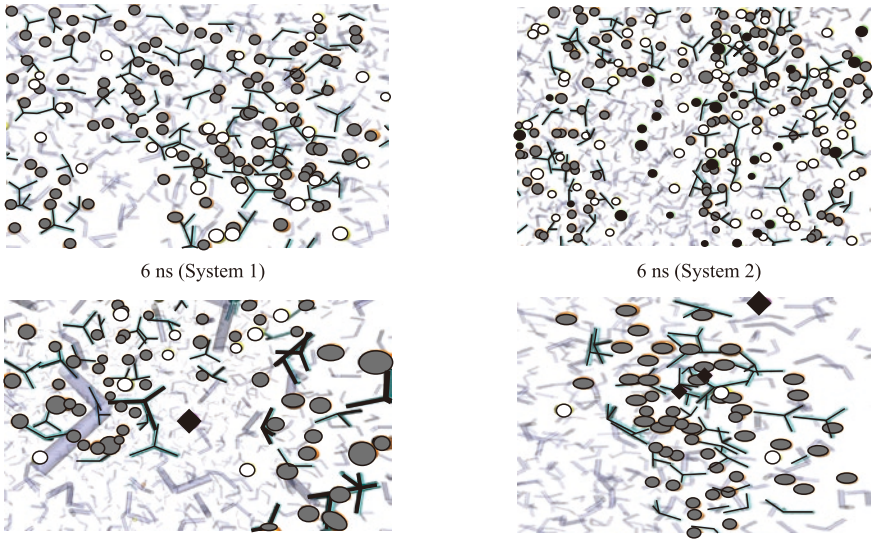

Fig.4 Schematic illustration of the simulation box(●-Li^+, ○-Na^+, ●-Cl^-, ◆-Mg^{2+}, — -H_2O, — -CO_3^{2-})

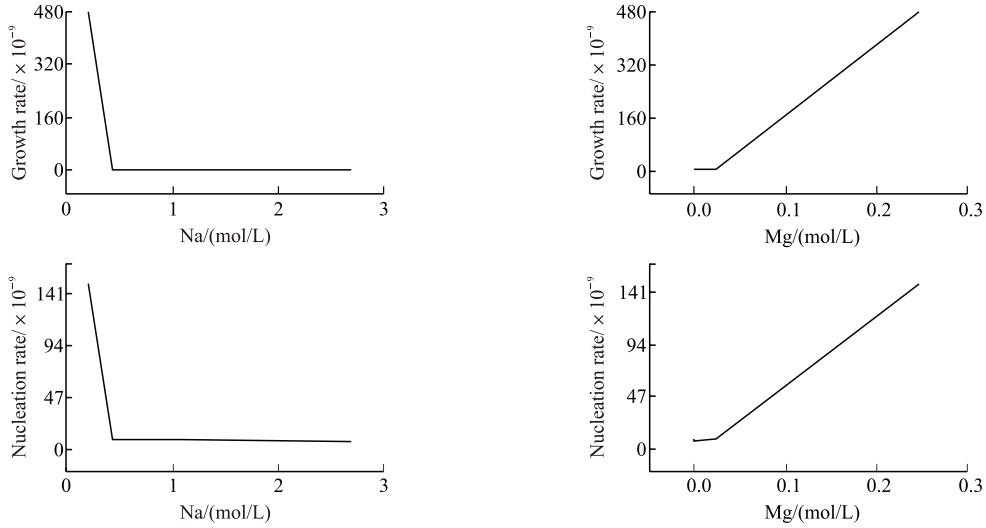

Fig.5 Effect of the impurity (Na and Mg) concentration on the nucleation and growth rates of the Li_2CO_3 crystals

of Mg^{2+}, with basically a linear relationship with concentration (Fig.5). The effect of Na ions was reversed.

Mg ions will limit Li-carbonate growth because of the formation of magnesium carbonate, causing solution supersaturation instability, and ventually affect the formation of lithium carbonate.

3.2.3 Radial distribution function and diffusion coefficient

The radial distribution function (RDF), also called pair correlation function, is the ratio between the atomic density in the system's local area and the average density of the system. It can help to understand the structure of molecular systems[21], especially the interactions between two atoms. The first peak position of $g(r)$ corresponds to the closest distance between two atoms, whereas its height and sharpness express the degree of structural order between them[22]. The results show that the Li–Li and Li–Na RDFs indicate that the height has a short-range ordered and a long-range disordered structure, that is, there are a small number of peaks with varying heights and sharpness at close distances; however the peak height rapidly decreases with the increasing distance. At long distances, the RDF tends to be evenly distributed, *i e*, $g(r) = 1$. The atomic arrangement and distribution exhibit no regularity in amorphous systems and the corresponding RDF usually shows only short-range peak positions; as the value range gradually increases and tends to infinity, its value tends to 1 and the atomic density in the local area becomes equal to the overall density.

Figs.6 and 7 illustrate the RDFs of Li–Li and Li–Na, respectively, in the four simulated systems, showing obvious differences between Li–Li and Li–Na; in particular, Li–Li was more ordered and stable than Li–Na. Due to the isothermal process, the crystallisation was slow and the system structure changed relatively slowly as well; as a consequence, the change of the Li–Li RDF is not clear. The peak of the Li–Na RDF was reduced to a certain extent and the first peak distance was larger than that for Li–Li.

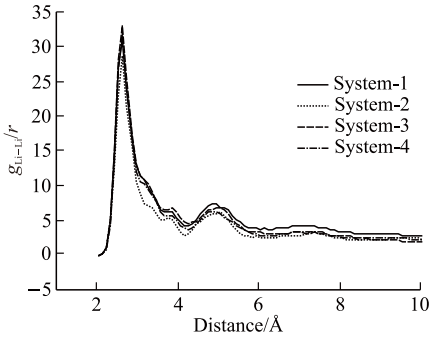

Fig.6 RDF of Li-Li

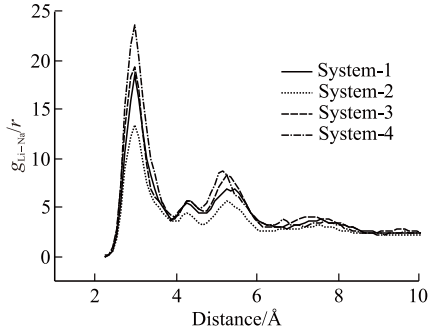

Fig.7 RDF of Li-Na

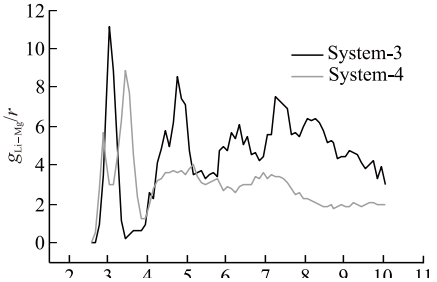

Fig.8 RDF of Li–Mg

Fig.8 displays the Li–Mg RDFs in system 3 and system 4. Due to the ordered structure of the crystal system, the RDFs presented peaks at both short and long distances and as the radius gradually increased approaching infinity, its value still fluctuated but did not tend to 1. The reported results show that Li–Mg had a poor order degree, the RDF had clear multiple peaks and the peaks were low, implying that the presence of Mg induced a certain degree of chaos in the system state, consequently increasing the disorder of the system particles and the number of Li–Mg peaks, which in turn, indicates that the crystallisation of Li and Mg was enhanced and could form relatively stable crystals. In addition, the SEM image (Fig.1(b)) confirms that the Mg ions were distributed only on the surface of the crystals formed by Mg itself.

The exact extraction method chosen for Li_2CO_3 production depends on the composition of the aqueous solution[23].

The significantly lower peak of the Li–Mg curve at 2.5–3.0 Å with respect to those of the Li–Li and Li–Na curves suggests a smaller number of CO_3^{2-} molecules around the Li and Mg atoms compared to those around Li–Li and Li–Na. The reduced binding probability of CO_3^{2-}in the system with H atoms in H_2O also confirms that Mg participated in the Li_2CO_3 crystallisation.

The comparison between the peak intensities of the Li–Li, Li–Na and Li–Mg RDFs reveals that the magnitude of the intermolecular forces followed the order Li–Li > Li–Na > Li–Mg and that both were larger than the hydrogen bonds.

The diffusion coefficient (D) is an important index

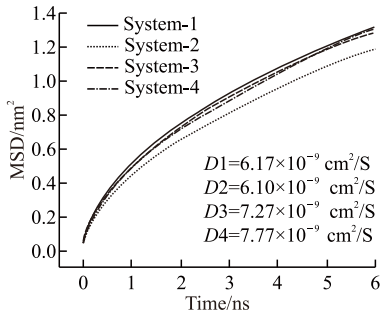

Fig.9 Mean square displacement of the four simulated systems

for measuring the diffusion capacity of particles and can be derived from their mean square displacement (MSD)[24], also called the squared particle displacement, which is calculated as follows:

$$\mathrm{MSD}=\langle|r_i(t)-r_i(0)|^2\rangle \quad (1)$$

where $r_i(t)$ is the position of the i^{th} particle at t, $r_i(0)$ is its initial position and N is the number of particles.As the real time interval for measuring D is extremely long in the case of the molecular translational motion, the limit at time (t) tends to infinity as follows:

$$D=\frac{1}{6N}\lim_{t\to\infty}\frac{d}{dt}\sum_{i=1}^{N}\langle|r_i(t)-r_i(0)|^2\rangle \quad (2)$$

By substituting the differential approximation in Eq.(2) with the ratio between MSD and time differential, that is, the slope (α) of the curve, D can be simplified as

$$D=\frac{a}{6} \tag{3}$$

Fig.9 shows the MSD of the Li ions in the four simulated systems at 353 K, along with the corresponding Einstein relationship coefficient and D calculated[25–27]. The results showed that diffusion coefficient is closely related to the salt content and temperature of the system. Under constant temperature, Simulation system 1-4 corresponding the Li ions D values were 6.17×10^{-9}, 6.10×10^{-9}, 7.27×10^{-9} and 7.77×10^{-9} cm^2/s respectively. The salinity influences the difficulty in diffusion. The salt content of the system has the greatest effect on the diffusion coefficient; as it increased, the diffusion of the Li ions was hindered and D significantly decreased, as shown in Fig.10. The Li ions D of system2, with higher Na ions content, was the lowest among the simulated systems.

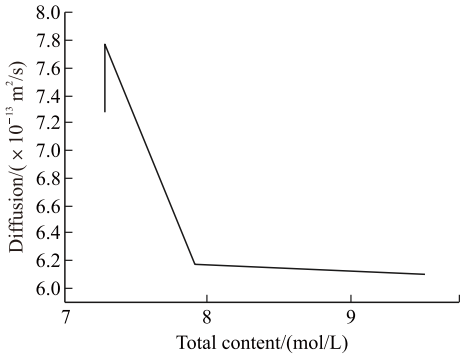

Fig.10 Diffusion coefficient of the four simulated systems

The diffusion rate was greater in the presence of Mg ions than that with Na ions, which suggests that the Mg ions destroyed the structure of the system solution to a greater extent. At the same time, the density of Na ions in the system was larger, resulting in stronger interactions with surrounding water molecules. The atoms became increasingly disordered and the value of D increased. This can be attributed to the difference of cations in the system.

4 Conclusions

The reported experimental study on the effects of Na and Mg ions on the Li_2CO_3 crystallisation, especially on the crystal quality and morphology, in salt lake brines has revealed a smaller contribution of the Na ions compared with the Mg ions. When the Mg ion content increased seven times, the grade of Li_2CO_3 decreased by twice of its initial value. Moreover, in the presence of Mg ions, the crystal morphology changed from rod-shaped to petal-shaped. The presence of the Na and Mg ions also broadened the Li_2CO_3 particle size distribution and decreased the average particle size.

Through molecular dynamics simulations, the effects of Na and Mg impurity ions on the nucleation and growth rates of Li_2CO_3 were further investigated; the Na ions slowed down the crystal nucleation and growth, whereas the Mg ions accelerated them and it was related to their concentration. Mg ions also participated in the crystallisation($MgCO_3$) along with the crystallisation of Li_2CO_3, while the Na ions did not crystallize and there was no precipitation of Na salts either, which is beneficial for the Li extraction from brine.

The presence of Mg ions made the Li–Mg RDF tending to be disordered and increased the diffusion coefficient. The diffusion rate was also greater compared with that in the presence of Na ions, which indicates that Mg ions can destroy the structure of the system solution to a greater extent. The comparison between the peak intensities of the Li–Li, Li–Na and Li–Mg RDFs revealed that the intermolecular forces followed the order Li–Li > Li–Na > Li–Mg and that were larger than the hydrogen bonds.

The results showed that the Na ions were adsorbed only on the surface of the Li_2CO_3 crystals, while the Mg ions also formed Mg salt crystals. Therefore, the role of the Mg ions in the Li_2CO system is far greater than that of Na ions, and therefore, the effects of impurities containing Mg ions on the Li_2CO_3 crystallisation should be systematically investigated in future works.

References

[1] Hao Yong, Zhang Qihai, Li Guanghan, *et al.* Synergistic Lithium Extraction from Mixed Brines of Jiezechaka and Longmucuo Salt Lakes in Tibet[J]. *Inorganic Chemicals Industry*, 2013, 45(6): 27-31

[2] Duan Shaojun, Sun Yuzhu, Song Xingfu. Study on Preparation of Lithium Carbonate Via Reactive Crystallization from Old Salt Brine[J]. *Shandong Chemical Industry*, 2018, 47(3): 5-13

[3] Nie Zhen, Bu Lingzhong, Wang Yunsheng, *et al.* Industrial Technology for Separation of Lithium from Magnesium Rich Salt Lake Brines[J]. *Inorganic Chemicals Industry*, 2013, 45(5): 1-4

[4] SONG Peng-Sheng, LI Wu, SUN Bai, *et al.* Recent Development on Comprehensive Utilization of Salt Lake Resources[J]. *Chinese Journal of Inorganic Chemistry*, 2011, 27(5): 801-805

[5] YU Jiangjiang,ZHENG Mianping,WU Qian. Research Progress of

Lithium Extraction Process in Lithium-containing Salt Lake[J]. *Chemical Industry and Engineering Progress*, 2013, 32(1): 13-21

[6] SONG Peng-sheng. Comprehensive Utilization of Salt Lake and Related Resources[J]. *Journal of Salt Lake Research*, 2000, 8(2): 33-36

[7] Wang Jishun, Gao Shiyang, Xu Kaifen, *et al.* Study on the Technoligieal Method for Extraetion Li_2SO_4 from Brine[J]. *Journal of Salt Lake Research*, 1994, 2(4): 31-34

[8] ZHAO Chunlong, SUN Zhi, ZHENG Xiaohong, *et al.* Research Progress of Lithium Carbonate Preparation and Purification Process[J]. *The Chinese Journal of Process Engineering*, 2017, 18(4): 8-14

[9] Kenta Ooi, Yoji Makita, Akinari Sonoda, *et al.* Modelling of Column Cithium Desorption from Li^+ -loaded Adsorbent Obtained by Adsorption from Salt Brin[J]. *e, Hydrometallurgy*, 2017, 169: 31-40

[10] Huaiyou Wang, Yuan Zhong, Baoqiang Du, *et al.* Recovery of Both Magnesium and Lithium from High Mg/Li Ratio Brines Using a Novel Process[J]. *Hydrometallurgy*, 2018, 175: 102-108

[11] Jeon Woong An, Dong Jun Kang, Khuyen Thi Tran, *et al.* Recovery of Lithium from Uyuni Salar Brine[J]. *Hydrometallurgy*, 2012(117-118): 64-70

[12] Helen E. King, Alistair Salisbury, Jasper Huijsmans, *et al.* Influence of Inorganic Solution Components on Lithium Carbonate Crystal Growth[J]. *Cryst. Growth Des*., 2019, 19, 6 994-7 006

[13] FengHai Liu, WenYan Tian, XiaoQing Yang, *et al.* Hydrogen-bonding and Dielectric Response of N, N-dimethylacetamide Aqueous Solutions Under E/M Fields Using Molecular Dynamics[J]. *Journal of Molecular Liquids*, 2014(197): 100-105

[14] Jianchuan Liu, Guozhu Jia, Zhou Lu. Dielectric Properties of Pyridine Derivative-Water Clusters: Molecular Dynamics Simulation[J]. *Journal of Molecular Liquids*, 2017(241): 984-991

[15] Wang J, Wolf R M, Caldwell J W, *et al.* Development and Testing of a General AMBER force Field[J]. *Journal of Computational Chemistry*, 2004(25): 1 157-1 174

[16] Jorgensen W L, Chandrasekhar J, Madura J D, *et al.* Comparison of Simple Potential Functions for Simulating Liquid Water[J]. *J. Chem. Phys*., 1983, 79 (2): 926-935

[17] Humphrey W, Dalke A, Schulten K. VMD - Visual Molecular Dynamics[J]. *Molec. Graphics*, 1996, 14: 33-38

[18] Mohammad Sheikh Hassani,Gholamreza Asadollahfardi,Seyed Fazlolah Saghravani, *et al.* The Difference in Chloride Ion Diffusion Coefficient of Concrete Made with Drinking Water and Wastewater[J]. *Construction and Building Materials*, 2020(231): 117 182

[19] Andrey O Doroshenko, Alexander V Kyrychenko, Oksana M Valyashko, *et al.* 4'-Methoxy-3-Hydroxyflavone Excited State Intramolecular Proton Transfer Reaction in Alcoholic Solutions: Intermolecular *Versus* Intramolecular Hydrogen Bonding Effect[J]. *Journal of Photochemistry & Photobiology A: Chemistry*, 2019(383): 111 964

[20] Li Wen, Wang Wensen, Zhang Yingnan, *et al.* Highly Efficient Water Desalination in Carbon Nanocones[J]. *Carbon*, 2018(129): 374-379

[21] Zhang Peng, Hou Dongshuai, Liu Qing, *et al.* Water and Chloride Ions Migration in Porous Cementitious Materials: An Experimental and Molecular Dynamics Investigation[J]. *Cement and Concrete Research*, 2017(102) : 161-174

[22] Dorota Swiatla-Wojcik,Joanna Szala-Bilnik. High Temperature Aqueous Solvent Effect on Translational and Hydrogen Bond Dynamics of the Hydroxyl Radical -MD Simulation Study[J]. *The Journal of Supercritical Fluids*, 2019(145): 103-110

[23] Liu X, Chen X, He L, *et al.* Study on Extraction of Lithium from Salt Lake Brine by Membrane Electrolysis[J]. *Desalination*, 2015, 376, 35-40

[24] FengHai Liu, WenYan Tian, XiaoQing Yang, *et al.* Hydrogen-bonding and Dielectric Response of N,N-dimethylacetamide Aqueous Solutions Under E/M Fields Using Molecular Dynamics[J]. *Journal of Molecular Liquids*, 2014(197): 100-105

[25] Chen Xia, Wang Yan, Wu Lianying, *et al.* A New Model in Correlating and Calculating the Diffusion-coefficient of Electrolyte Aqueous Solutions[J]. *Fluid Phase Equilibria*, 2019(485): 120-125

[26] XU Bing, LIU Cun, ZHOU Dong-mei, *et al.* Molecular Dynamics Simulation of Metal Ion-lipid Bilayer Interactions[J]. *Journal of Agro-Environment Science*, 2019, 38(7): 1 482-1 489

[27] YANG Wei, CHEN Ren-peng, KANG Xin. Application of Molecular Dynamics Simulation Method in Micro-properties of Clay Minerals[J]. *Chinese Journal of Geotechnical Engineering*, 2019, 41(1): 181-184